Journal of Renewable and Sustainable Energy | ARTICLE | pubs.aip.org/aip/rse

Modeling and control of nuclear–renewable integrated energy systems: Dynamic system model for green electricity and hydrogen production

Cite as: J. Renewable Sustainable Energy **15**, 046302 (2023); doi: 10.1063/5.0139875
Submitted: 24 December 2022 · Accepted: 20 June 2023 ·
Published Online: 7 August 2023

Roshni Anna Jacob and Jie Zhang[a)]

AFFILIATIONS

The University of Texas at Dallas, Richardson, Texas 75080, USA

Note: This paper is part of the special issue on Hybrid Renewable Energy Systems.
[a)]**Author to whom correspondence should be addressed:** jiezhang@utdallas.edu

ABSTRACT

The need for decarbonization and diversification of energy resources has led to the development of integrated energy systems (IESs), where multiple resources supply more than one energy sector. One such IES with small modular nuclear reactors and renewables (wind and solar) as generating resources, catering to the demand of the electric grid while producing hydrogen for industries, is modeled in this paper. The physics-based component models are represented using the Modelica language and interconnected to form the IES. The control and coordination of the overall system are ensured by designing a suitable control architecture composed of individual subsystem-level controls and supervisory control. The dynamic performance and the load-following capability of the IES are evaluated, while satisfying the safe operational limits of the components. Different configurations and modes of IES operation are considered, where the adaptability of the control system in the presence of varying demands and renewable generations is validated. The simulation results indicate that hydrogen as a flexible load facilitates the supply of varying grid demand. Additionally, the renewables are also accommodated into the IES owing to the flexibility of the balance of plant associated with the nuclear reactors.

I. INTRODUCTION

There has been an unprecedented transformation of the energy sector during the past few decades, which can be attributed to factors such as growing concern for climate change, rapid depletion of fossil fuel reserves, and increasing penetration of renewable energy resources. Contemporaneously, the escalating frequency of anthropogenic outages and the energy crisis arising from socio-political events have emphasized the need for improving the national energy security and resilience. Considering this, the course for the future adopted by the global energy industry is decarbonization and diversification. The former can be achieved by utilizing energy resources such as solar, wind, and nuclear energy that do not produce greenhouse gas emissions. The latter, on the other hand, has led to a conceptual change in the energy sector and resulted in the promulgation of integrated energy systems (also known as hybrid energy systems).

An integrated energy system (IES) is one that couples multiple energy resources, such as nuclear and renewables, to provide energy supply for different sectors (e.g., electricity, heating, and hydrogen), by using complementary conversion processes on the primary form of energy.[1] The IES is the term coined for the holistic approach of integrating multiple energy sectors that are traditionally considered independent.[2] These systems enable economic and efficient use of the input energy, including the clean energy resources.[3] For example, rather than curtailing nuclear generation or riding through negative profits in the electricity market, in an IES, the energy (both thermal and electrical) can be diverted toward other end products, which are more desirable. By replacing the traditional one-to-one source-product pairing, the IES provides flexibility in energy management, while also effectively accommodating intermittent and non-dispatchable renewable energy resources without compromising on the grid reliability.[2]

The IES may have a tightly coupled or a loosely coupled configuration.[4] In a tightly coupled IES, the multiple energy resources (subsystems) are coordinated and controlled as a single entity, are often co-located, and have one point of connection with the electrical grid. On the contrary, the loosely coupled IES consists of resources that are distributed at different points within the energy network (which may be electrical or thermal). These are, however, controlled in a coordinated manner by a single management or operator to ensure that the demand is supplied through optimal scheduling and dispatch. The configuration and the objective of the IES are dependent on the geographical conditions, resource availability, and the needs of the locality in which it is set up.[5] For instance, hydrogen production may be desirable as an industrial process in areas with oil refineries, while desalination may be the requirement in desert or coastal areas. Additionally, IES may be particularly useful in remote locations where it can be designed to meet all the energy requirements of the area in a stand-alone, off-grid manner.[1] In this respect, the development of small modular reactors (SMRs), a form of advanced nuclear reactor, is considered to be a significant development that further promotes the notion of IES. The flexible and modular nature of SMRs as a clean-energy resource facilitates localized energy production with ease of transport and scalable installation at selected sites.[6] In this paper, we consider SMRs and renewables in parallel as the primary energy resource, and the IES to be tightly coupled.

Alongside the development of SMRs, another stimulus for the IES is the promotion of green hydrogen generation, storage, and consumption facilities by the U.S. Department of Energy (DOE).[7] The H2@Scale initiative launched by the DOE promotes clean hydrogen production, distribution, storage, and utilization with the aim of decarbonizing and opening new revenue streams in the energy sector.[8] As a part of this initiative, the production of hydrogen from diverse resources and its utilization in multiple energy sectors are considered, which may progressively lead to the adoption of more IES facilities. Hydrogen as an energy carrier is a necessary feedstock in several industrial applications, such as in chemical production and manufacturing, and power generation, and it is also used as fuel for transportation. Additionally, it is also a suitable means of energy storage and, therefore, aids in accommodating renewable energy resources. The hydrogen production using electrolysis, specifically high temperature steam electrolysis (HTSE) and low temperature electrolysis, has been discussed in the literature with studies on challenges[9] and integration with nuclear reactors.[10] Several researchers have also performed optimal scheduling,[11,12] techno-economic analysis,[13,14] and resilience studies[15] on IES. In addition to this, dynamic modeling and control of IES with district heating networks[16,17] have also attracted much attention from the research community.

An IES is a complex system that requires safe and coordinated operation of multiple components. Also, the energy and material flows within the system are dynamic in nature. Therefore, to analyze the overall system behavior and to evaluate the feasibility of different configurations and operational scenarios, a dynamic study is pertinent. One such dynamic study would require a physics-based representation of the system along with the modeling of control architecture. Given that the IES is a "system of systems" with material transfer and interaction between different forms of energy, a multi-domain tool with hierarchical modeling capability is required to represent the physical system. The Modelica language[18] is a suitable tool as it aids in multi-domain modeling with acausal equation-based mathematical representations for the relationship between component variables. Complex multi-domain problems of dynamic nature can be solved using the numerical solvers available in the software with sufficient fidelity and reasonable performance. One of the most desirable features of the Modelica language is the object oriented programming nature; thus, the inheritance property, which facilitates developing components derived from existing models, with further extension or modification of the behavior, is derived.[19] In our modeling efforts, several base models derived from different packages or libraries have been utilized with the addition of new properties, data, and functionalities (control strategy) to create required component models in the IES using inheritance.

With the prospect of facilitating dynamic modeling and prototyping nuclear based IES, the Oak Ridge National Laboratory (ORNL) developed the *TRANSFORM*[20] library using the Modelica language. Along with the physical model description of different kinds of nuclear reactors, it also put forward a template for modeling future IES designs. Following this, in early 2013, the Idaho National Laboratory (INL) initiated the development of high fidelity models for IES components using the Modelica language in the Dymola platform.[21] These models are now opensource and available as the NHES package in the Hybrid repository.[22] Different models for reactors, energy conversion based on Rankine cycle, industrial plants, etc., have been added onto the initial ORNL template.[23–25] Capitalizing on the developed physical models, Garcia *et al.*[1,26] performed dynamic modeling and evaluation of two particular IES architectures for specific regions in the U.S. with a nuclear reactor as the primary energy resource. The first IES configuration considered is in West Texas with nuclear, wind, and natural gas as resources, and with electricity, and gasoline as end products. The second IES located at Northeastern Arizona is comprised of nuclear and solar resources for electricity production and desalination. In both IES models, physical representations and control modeling of wind and solar plants were ignored, and a simplistic functional mapping of wind speed or irradiance to power output was adopted. Additionally, hydrogen production as an industrial process was not considered here since the specific case studies did not warrant a hydrogen plant due to geographical conditions, policy, and regulatory reasons. Furthermore, Chen *et al.*[27] performed optimal operation scheduling studies for the aforementioned regional cases with the objective of maximizing revenue and minimizing costs considering the variability of renewable generations and electricity markets. For the IES case study involving the Arizona Public Service, Epiney *et al.*[28] performed economic assessment of the IES operation using a framework built using the Risk Analysis Virtual Environment (RAVEN) tool. Another component in this framework is the reduced order model of the brackish water reverse osmosis desalination plant, which is derived from its corresponding physical representation in Modelica. In the recent years, INL has also designed and installed the dynamic energy transport and integration laboratory (DETAIL) for demonstrating the integration of different components (such as the grid and renewable energy) and interoperability between thermal and electrical energy conversion processes in real-time.[3] A component embedded within the proposed DETAIL infrastructure is the thermal energy distribution system (TEDS), which is used to validate the interaction between the reactors, thermal storage, and the control mechanisms. Frick *et al.*[19] developed a detailed model of the TEDS in Modelica for testing the technical feasibility and the synergy between components.

A high fidelity model for hydrogen production using the high temperature steam electrolysis has been added to the NHES/Hybrid package as an industrial plant.[29,30] With this, Kim *et al.*[31] evaluated the hydrogen plant dynamic behavior in an IES with varying parameters. However, in this work, the focus was on the HTSE plant rather than the control and coordination of the overall system. Also, the renewable plant behavior and associated control was also not sufficiently captured. To facilitate the development and testing of advanced HTSE technologies, a flexible test station that evaluates 25 kWe SOEC stacks has been deployed at INL.[32] The objective of the facility is to improve the HTSE stack technology and to enable demonstrations of the dynamic operation and control in a thermal-electrical coupled system. At INL, various hydrogen production systems of different scales are under development or already set up for testing.[33] Among these systems is the 100 kW high-temperature electrolyzer by Bloom Energy, which includes multiple cell stacks and other equipment that support the hydrogen production process such as hydrogen separation from steam and cooling mechanism. The Bloom Energy electrolyzer has already completed 500 h of full load operation at INL[34] with efficiency in hydrogen production higher than the commercially available alkaline and proton exchange membrane (PEM) electrolyzers. A pilot study was conducted to assess the performance of the HTSE in a thermal-electrical system by integrating it with the DETAIL facility, emulating the steam and load conditions of hydrogen systems that complement nuclear power stations. The HTSE system also demonstrated good dynamic performance by ramping from 100% to 5% of rated power in less than 10 min without significant impact or degradation of the system state. Pinsky *et al.*[35] compared the different water-based hydrogen production technologies to promote its integration in IES. According to this study, HTSE is suitable for integration with nuclear plants due to the range of its operating temperature, and it is much cheaper despite the technology being not mature. Consequently, a pilot study to evaluate the economic feasibility of re-purposing a light water reactor in the Illinois region for hydrogen production using HTSE was launched.[36] The results of this study indicate that the revenue of the nuclear plant could be increased by operating HTSE at full capacity or in hot standby mode when the electricity price is high. Recently, Ulrich *et al.*[37] designed and tested a data connection between the IES including a HTSE pilot plant and the human operator systems to bolster the development of control and communication for implementing such systems. As is evident from the developments discussed, hydrogen production within IES is undoubtedly gaining prominence.

Recognizing the need for physical models of IES with clean energy resources for green electricity and hydrogen production, in this paper, we present the dynamic model, design of control architecture, and the evaluation of the system behavior with various configurations and modes of operation. The physics based models using the Modelica language are developed to emulate the actual behavior of components and, therefore, functions as a prototype for validating the IES. In our paper, we also demonstrate the load following capability with varying demand and renewable generation while ascertaining operational feasibility. Other significant contributions of this paper include the following:

- Investigation of the system behavior with intermittent and non-dispatchable renewable energy.
- Evaluation of the dynamic control of the IES and its components while responding to variations in demand and atmospheric conditions.
- Validation of the coordination between subsystems and ensuring flexibility in energy management by apportioning energy to multiple pathways/processes.

The remainder of this paper is organized as follows: The individual component models within the IES are discussed in Sec. II. Section III discusses the overall control framework including the component control strategy. Following this, in Sec. IV, different configurations and operational modes are presented with results and discussion of findings. Finally, the conclusions and future work are discussed in Sec. V.

II. INTEGRATED ENERGY SYSTEM COMPONENTS

The IES components are described using the Modelica language in the Dymola simulation environment. The physical models available in the *Hybrid/NHES* package are extended and modified using the object-oriented modeling capability offered by Modelica. We adopt the template provided by ORNL and insert component models into the sandboxes. Therefore, each component in the IES is modeled as a subsystem that can function in a both standalone and integrated fashion. In addition to the components within the NHES package, we also utilize two other libraries for renewable plant modeling, namely, *WindPowerPlants*[38] and *PhotoVoltaics*.[39] In this paper, we have considered the nuclear power plant as the primary heat-generating system, and hydrogen production as the industrial process. Additionally, the renewable energy subsystem added to the IES may be a wind power plant or a solar power plant. The overall IES architecture is presented in Fig. 1. As seen in the figure, the physics of the component models and the thermal-hydraulic and electrical flows are represented by the model. In this section, we will briefly discuss the component models used within the IES.

A. Small modular reactor (SMR) plant

The nuclear reactor is the primary energy resource for all the IES configurations considered in this paper. As such, the thermal energy required to drive the turbine-generator for electricity generation and to produce the steam for electrolysis is generated from the nuclear process. The nuclear plant model adopted in this paper is a generic modular pressurized water reactor model derived from the *TRANSFORM* library. A single module is rated at 160 MW thermal with an electrical equivalent of 50 MW.[21] Three such modules in parallel constitute the primary heat supply system in this work.

The reactor module is composed of a primary and a secondary coolant loop on the shell and tube side of a steam generator. The primary coolant that enters the reactor core through the cold leg is heated by the nuclear reaction and exits through the hot leg while moving through a riser with a pressurizer and flowing down through the steam generator.[2] The function of the pressurizer is to maintain the pressure of the primary coolant at nominal values. The thermal energy is further carried by the vapor that is superheated by the heat transfer from the primary coolant to the secondary in the steam generator. The secondary pump can be controlled to regulate the differential temperature. The reactor core dynamics including the core neutronics, the helical coil steam generator, the pressurizer behavior,[21,23] etc., have been modeled using mathematical representations in *TRANSFORM*.

B. Balance of plant (BOP)

The balance of plant (BOP) converts the thermal energy, which is directed toward the electricity generation process using a turbine-generator set, into electrical power. The steam inflow to the BOP is directed toward the turbine through a turbine control valve (TCV), which then flows into the condenser. The remnant steam is diverted directly toward the condenser through the bypass valve (BV).[21] The industrial plant return supply is also dumped into the condenser. The condensed fluid is then returned back to the secondary loop within the steam generator in the reactor modules. The bypass valve control is vital for maintaining the pressure within the secondary loop.

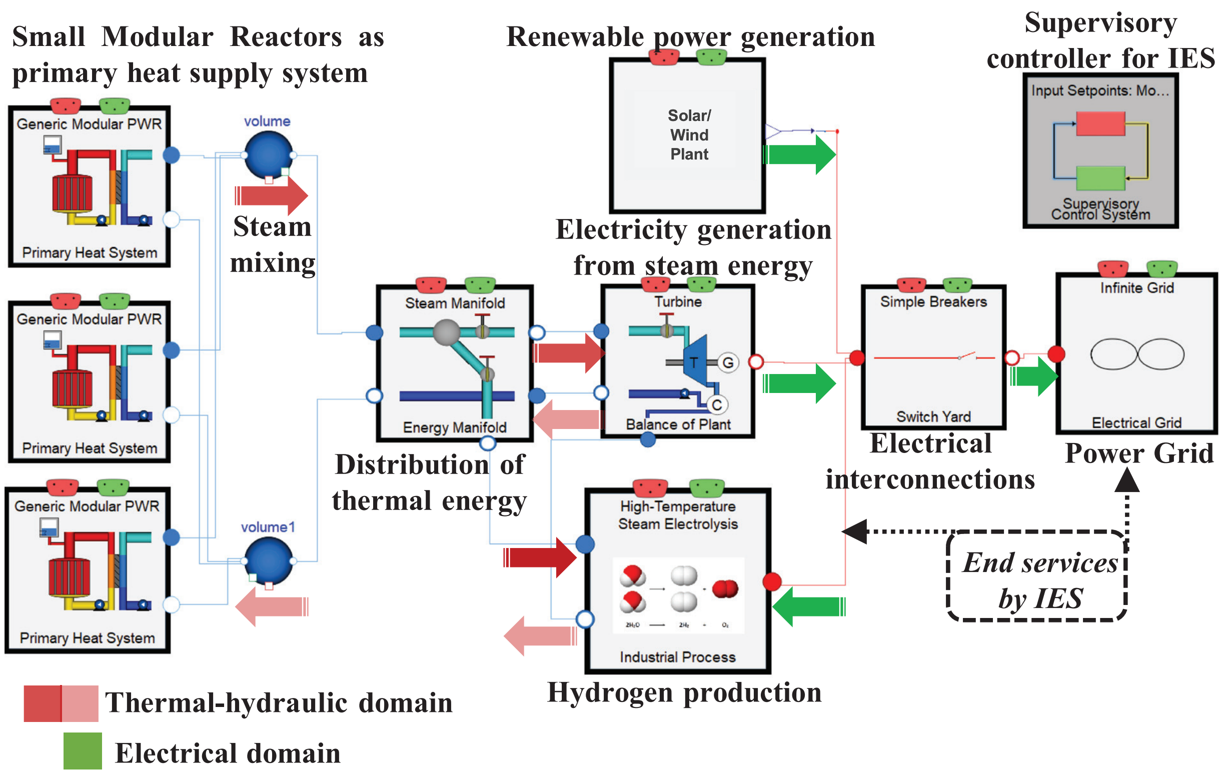

FIG. 1. Top level view of the IES model in Dymola with component definition.

C. High temperature steam electrolysis (HTSE): hydrogen production

A high temperature steam electrolysis (HTSE) plant can exploit the high temperature steam from the nuclear plant to split water into hydrogen and oxygen in the presence of electricity. This process is the reverse of that in the solid oxide fuel cells and takes place in solid oxide electrolyzer cell (SOEC) stacks, which are three-layer structures that consist of a porous cathode, anode, and electrolyte with a separator plate. The steam inflow to the HTSE is split into two streams, one for the cathode and the other for the anode. The cathode stream transfers the thermal energy to a feedwater, which is further superheated before passing onto the cathode.[30] The anode stream, on the other hand, transfers heat to an airflow. The two streams are further combined to form the return supply from the HTSE. The steam at 850 °C, mixed with hydrogen, is provided to the SOEC stacks on the cathode where it is reduced into hydrogen by electrochemical reactions. The steam utilization factor is set at 80% to avoid performance degradation, and the exit temperature is 750 °C.[31] The residual steam on the cathode stream is condensed to remove heat. The oxygen enriched air on the anode stream is the outlet of the SOEC stacks.

The cathode and the anode stream inlet into the SOEC is required to be at 850 °C for the HTSE process. However, the steam directed from the energy manifold toward the HTSE meets only a fraction of the heat required for the electrolysis (typical temperature is 300 °C). Therefore, the stream is further heated with a topping heater using electricity. The remaining electricity is then supplied directly to SOEC stacks for electrolysis. The HTSE model in the NHES package is suitable for light water reactor (LWR) technology. The steam conditions of this model along with other parameters (e.g., return pump pressure) have been modified for integration with SMRs.[24]

D. Energy manifold (EM) for thermal energy distribution

The energy manifold (EM) or the steam manifold is used for distributing the steam into different streams as per the objective or requirement of the IES. For example, in the case of an IES producing both electricity and hydrogen, the steam inlet to the EM from the SMR modules is apportioned between the BOP and the HTSE to meet the demand. The EM essentially consists of pipes, splitting volumes, and valves to direct the flow toward the desired process, i.e., electricity generation or hydrogen production. Furthermore, the return flow from these streams are also mixed and directed back toward the secondary of the SMR steam generator at nominal pressure and temperature. The valves in different streams are actuated by the control module, which is user-defined and varies with IES functionality.

E. Wind power plant

The wind power plant in the IES is developed using the open source *WindPowerPlants*[38] Modelica library. This library contains component models such as the wind turbine and variable speed generator for modeling a single wind power generating unit. Several such units are aggregated using suitable descriptions in Modelica to represent a wind plant in the IES. The wind speed is fed in as real data into the model, which is converted using an adaptor to speeds suitable for the turbine height. The total kinetic energy possessed by the wind is estimated from the wind speed, with only a fraction being converted by the turbine.[38] This fraction characterized by the power coefficient is dependent on the turbine design and pitch angle. The pitch angle is used to control the converted power (discussed in Sec. III E). These relations and other turbine characteristics are described using mathematical representations in the Modelica language. A generic variable speed generator, which converts the mechanical power to electrical power, is available in the *WindPowerPlants* library. The reference torque for the generator is determined by the angular velocity control. The wind turbine data available within the library is utilized in our IES model as well. The wind plant modeling takes into account the electromechanical transients; however, the electrical transients are not captured here. This can be ignored as the other component models in the IES are modeled with the objective of controlling the energy and material flow between different subsystems while ensuring the conservation principle. The focus of our paper is multi-domain energy management and control during normal operations. The model is developed with the aim to assess the technical feasibility of incorporating multiple end products, varying demands, and renewable energy generation. Hence, the dynamic response of this multi-domain complex interconnected system is intended to effectively capture only the slower transients caused due to the mismatch in power generation and consumption. Therefore, the wind power plant model is in congruence with the other subsystems in this regard.

F. Photovoltaic solar power plant

The solar plant in the IES is represented using physical models available in the open source *PhotoVoltaics*[39] library. This library includes models for components such as photovoltaic (PV) cells, modules, power converters, maximum power point trackers, and irradiance data adaptors. The PV module data sheet values for the open circuit voltage (OCV), short circuit current (SCC), maximum power voltage and current, and linear temperature coefficient of OCV and SCC, all at reference conditions available in the library, are directly used in our IES solar plant model. The PV cells are represented using diodes and a current source with the source current expressed as a function of the irradiance and the temperature. The different aspects of the physical PV cells such as the OCV, SCC, and temperature dependencies are effectively captured in component descriptions in the library. The PV modules are connected in parallel and in series combinations to develop a plant. For M_P modules in parallel and M_S in series, the plant current is $M_P * i_{cell}$ and the plant voltage is $M_S * v_{cell}$, where i_{cell} and v_{cell} are the current and voltage of the PV cell, respectively. A quasi-static multi-phase (here three-phase) converter model is available for converting the DC power to three-phase AC power suitable for grid interconnection. The DC reference voltage in the converter DC side is provided by a maximum power point tracker.

G. Switch yard (SY) and electric grid (EG)

The switch yard houses the point of electrical coupling between the IES subsystems and the grid. The different components are connected using switches, which can also be controlled if required. In our IES configurations, the BOP, wind plant, solar plant, and the HTSE are connected to different input ports with the grid on the output port. Among these, the first three subsystems are generators, while the HTSE acts as an electrical load. The grid is modeled as an infinite source/sink in the Hybrid/NHES library, which is directly used in our IES model to represent large grid behavior.

Each of the subsystems discussed here are accompanied by individual control modules which are presented in Table I and will be elaborated in the Sec. III.

III. CONTROL OF THE INTEGRATED ENERGY SYSTEM

The IES is essentially an interconnection of different components, with each component required to operate within safe limits while working in tandem with each other to achieve the desired global behavior. The objective of the IES in different configurations is to meet the various demands which are defined as the desired global behavior in the supervisory control. The individual control modules within each subsystem control local components such as pumps, valves, and

TABLE I. A summary of the primary control modules for different components in the IES. The measurements are acquired using sensors and relayed to control modules. The control signals are then transmitted from the module to the control elements.

Components	Measurements	Control signals	Control elements
SMR	Thermal power output, core differential temperature	Reactivity, mass flow rate	Control rod, secondary side pump
EM	Mass flow rate to HTSE	HTSE and BOP stream valve opening[a]	Valves
BOP	Electric power generated, secondary loop pressure	TCV and BV opening or position	Valves
HTSE	Temperature of cathode and anode stream[b],	Valve opening or position	Valves,
	power consumed[c]	Modulating signal	Power converter (load impedance)
Wind plant	Angular velocity or rotor speed	Pitch angle, torque	Pitch motor, power converter
Solar plant	Solar plant power	DC voltage reference (MPPT control)	Power converter

[a]Only in power control mode of HTSE.
[b]Steam control mode.
[c]Power control mode.

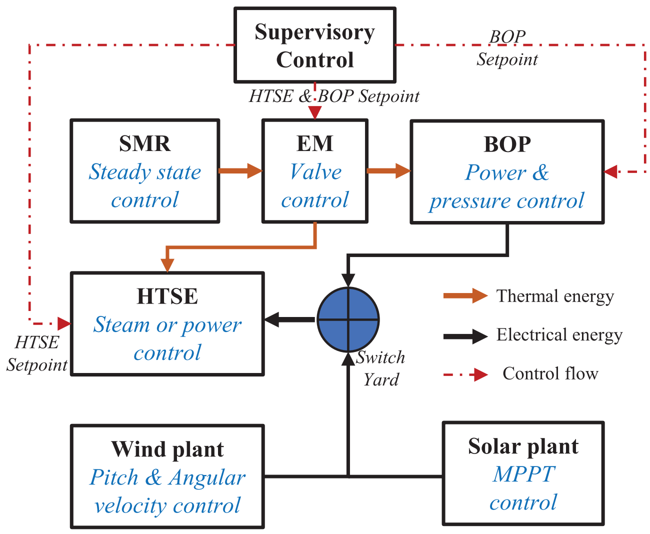

FIG. 2. Architecture for the coordinated control of IES components.

switches in a dynamic fashion to follow the setpoint assigned by the top level supervisory control. The architecture of the control system with the modes of control in each subsystem is described in Fig. 2. The template provided in TRANSFORM (ORNL) and Hybrid/NHES (INL) has sandboxes for the control modules with sensor and actuator buses. We design the IES control using this template with the modified control system assigned to each component that is suitable to the configuration and mode of operation. The various signal measurements are relayed to the controls using the sensor bus, while the control signals are transmitted through the actuator bus to the control elements

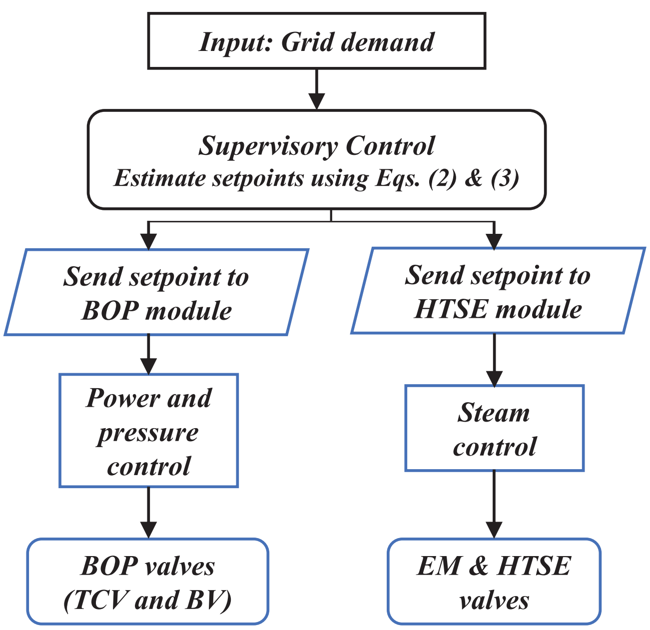

FIG. 3. Flowchart representing the control strategy implemented with grid demand available to supervisory controller.

(such as valves and pumps). The control strategy for the IES with nuclear and renewable energy resources generating electricity and hydrogen as end products is presented in Fig. 3.

A. SMR control

The SMR units are each assigned a control module to monitor and control the individual plant operation. The control module consists of the traditional PI controllers that ensure that the plant generates the desired primary heat while adhering to operational constraints and safe limits.[24] The desired thermal power is provided as the set point to the control module of the nuclear reactor, which functions to adjust this accordingly. The variation in reactor thermal power output is, however, less frequent (seasonal or planned for events), and the plant is often made to operate at full load capacity. It is desirable to operate the nuclear reactors at steady state, while relying on the BOP and hydrogen generation (by HTSE) to provide the much needed flexibility in meeting grid demand by the IES. This is owing to the efficient use of capital investment and nuclear fuel with operation at rated thermal power while minimizing degradation (reduced maintenance) and safety concerns.[40]

The steady-state control module for the SMR encapsulates the thermal power control and the secondary side coolant flow control. The thermal power of the SMR is monitored and is set to the desired value by varying the reactivity of the core using a PI controller. Reactivity is the fractional change in neutron population dependent on generation and is an indicator of deviation from criticality (zero reactivity). In addition to this, the differential core temperature (i.e., the difference between the hot leg and the cold leg) is regulated at a preset level (here 39 K) by using a PI controller to drive a feedwater pump in the secondary of the steam generator, which in turn proportionally affects the heat transfer from the primary coolant to the secondary coolant and, thus, the heat removal from the nuclear fuel.

B. EM control

The function of the energy manifold is to divert the thermal energy to the different energy conversion processes in the IES as per the demand. In our case studies, we consider electricity and hydrogen generation as the end products. Hence, the EM is composed of pipes and valves to apportion the steam to the BOP and HTSE dynamically as per the set points generated by the supervisory control.[21] The EM control model used extensively in Hybrid/NHES consists of virtual boundaries (with source and sink), which emulates the inlet and outlet steam conditions of the HTSE and a direct supply and connection to the BOP. This form of decoupled control modeling works in conditions where the electricity generation is the primary objective of the IES, and the hydrogen is considered as a flexible energy resource. Additionally, the mass flows to the BOP and HTSE are already controlled by their respective control modules. Hence, the Modelica solver attempts to automatically equate the mass flows to the two streams within the EM accordingly, and no particular control is designated.

On the other hand, if we desire to directly control the steam mass flow rate into the HTSE (discussed in HTSE power control mode), valve controls are utilized. The valve opening position (0 to 1) is adjusted by using a PI controller with the actual mass flow rate controlled to achieve desired steam input into HTSE. The opening of the valve in the stream toward BOP is directly opposing the change in HTSE stream valve since $m_{EM} = m_{HTSE} + m_{BOP}$ (considering the same specific enthalpy and pressure).

C. BOP control

The BOP is responsible for the conversion of thermal energy from the nuclear process to electricity that is used for different applications in the IES. The two valves in the BOP, namely, the turbine control valve (TCV) and the bypass valve (BV) are controlled by the BOP control module which encompasses two PI controllers corresponding to each valve actuation. The TCV permits the steam flow toward the turbine-generator set for electricity production, which is directly proportional to the electricity demand on the BOP set by the supervisory control. The BV, on the other hand, allows the remnant of the steam energy to flow toward the condenser before feeding it back through the EM to the secondary of the steam generator within the SMRs. The BV regulates the pressure in the secondary loop of the steam generator and also indirectly maintains the primary coolant average temperature. Hence, the control within BOP is called power and pressure control.

D. HTSE control

The high temperature steam electrolyzer (HTSE) has two modes of control depending on the input and the control variable. If the steam input to the HTSE is predefined by the external optimizer (or assigned for the IES operation by the supervisory control), the corresponding electric power consumed is controlled and, hence, is called the power control mode. In contrast, for the steam control mode, the opposite is true. The electric power available for consumption by the HTSE is defined by the top level supervisory control and, hence, the steam input, i.e., the mass flow rate, is controlled. In most IES configurations, the electricity generation is the primary goal, while hydrogen is used as the flexible electrical load. Hence, in these circumstances, it functions in the steam control mode.

In the steam control mode, the electric power available for the HTSE is predefined. As mentioned earlier, the steam utilization factor is maintained at 80% in the SOEC.[30] Corresponding electrical energy is used in the SOEC stack. The remaining electricity is used for heating streams in the topping heater. This means that the degree of freedom is in the temperatures of the cathode and anode stream. A PI controller is used for achieving the desired temperature by actuating valves on both the anode and cathode stream. These temperature control valves, thus, vary the mass flow rate through both the streams, which in turn affects the HTSE inlet and outlet.

In the power control mode, the mass flow rate of the steam input to HTSE is predefined. The anode and cathode stream also varies in accordance with the input flow rate. This indicates that in order to achieve sufficient temperatures, electric heating is required to be controllable. Therefore, in this mode, the electric power consumed by the HTSE is controlled to support the steam electrolysis process.

E. Wind plant control

The wind plant model from the *WindPowerPlants*[38] library is accompanied by built-in controls, specifically, the pitch control and the angular velocity control. In the pitch control module within the turbine, the control for two different ranges of operation is described using logical operators and mathematical equations. In the optimal power coefficient range, the pitch angle β is determined from the polynomial function expressed as

$$c_p = c_1\left(\frac{c_2}{\lambda_i} - c_3\beta - c_4\right)e^{-\frac{c_5}{\lambda_i}} + c_6\lambda_i, \tag{1}$$

where c_p is the power coefficient, λ_i is the internal wind tip ratio, which is a function of tip speed ratio, and $c_1, c_2, .., c_6$ are coefficients (in per unit) that depend on turbine design. The estimated pitch angle (β) is further limited to be within 0° and 90° with a first order delay to obtain smooth pitch angle. In the power limiting range, a fast limiting integral controller is used for pitch angle control to ensure that the power produced does not exceed the maximum power specified for the turbine model.

The angular velocity control module is used in the generator component and describes the control during operation in both the standstill region (wind speed less than cut-in) and power generating region. In the standstill region, the reference angular velocity is set as zero with the reference tip speed ratio also at zero. On the other hand, in the power generating region, the tip speed ratio is set to reference tip speed ratio estimated for the optimal power coefficient (c_p). The tip speed ratio is determined with angular velocity ω, wind speed v, and rotor diameter D, using $\lambda = \frac{\omega D}{2v}$. The deviation in tip speed ratio is directly related to the deviation in angular velocity, which is used by the PI controller to set the torque reference for the generator.

F. Solar plant control

To utilize the full potential of solar energy conversion, the PV plant is operated at the maximum power point. This requires a maximum power point tracker (MPPT), which controls the DC voltage on the PV side of the power converter. The power of the plant is sampled at finite sampling intervals, and the voltage is changed to follow the changes in maximum power point. The voltage is initialized and then decremented. In case the power measured exceeds that of the previous sample, the voltage is further decremented. This is done iteratively and once the power at current sample is less than the previous sample, the voltage is incremented till it exceeds the maximum power point. This is available as a code block or function in the *Photovoltaics* library.[39] The output of the maximum power point control is the voltage, which functions as the DC reference of the converter.

G. Supervisory controller (SC)

The supervisory controller is responsible for energy management within the IES and coordinates the different subsystems to meet the demand on the system. The control strategy represented in Fig. 3 is implemented within the supervisory controller. The SC generates setpoints for the different IES subsystems. The setpoint for the nuclear reactor modules is the thermal power output, while the electrical power output is the setpoint of the BOP. Although, the HTSE utilizes both thermal energy and electricity, the setpoint in consideration is the electrical power consumed by the hydrogen plant. The SC determines the setpoint for HTSE using the following equation:

$$HTSE_{\text{setpoint}} = \lim(BOP_{\max} + P_{\text{Renew}} - \sigma HTSE_{\text{therm}} - P_{\text{Grid}}). \tag{2}$$

Here, $BOP_{\max}$ is the maximum capacity of BOP, $HTSE_{\text{therm}}$ represents the thermal rating of HTSE, σ is the thermal-electrical energy conversion factor, P_{Grid} represents the grid demand, and the renewable power (if present in IES) is represented by P_{Renew}. The lim represents the limits on HTSE power, which is 21 MW (lower) and 51 MW (upper). Furthermore, the BOP setpoint is estimated as

$$BOP_{\text{setpoint}} = P_{\text{Grid}} + HTSE_{\text{setpoint}} - P_{\text{Renew}}. \quad (3)$$

As seen in the control architecture (Fig. 2), the supervisory controller determines the setpoints for the operation of the components within the IES and transmits it to the lower level controllers in each module. This takes the form of a master-slave architecture with the supervisory controller in the role of the master. The assumption while designing the control architecture is that the IES is tightly coupled with a single point of interconnection with the grid. Hence, from the grid perspective, the IES is a generating resource. As with other generating resources in the grid, an optimal scheduling and dispatch tool determines the generation required from the IES depending on the economics. This demand on the IES by the grid is the input demand provided to the supervisory control in our model.

IV. SIMULATION RESULTS AND DISCUSSION

To evaluate the dynamic behavior of the IES and validate the load following capability in the presence of the varying demands and renewable generation, we consider different configurations and operation scenarios for simulation. Table II briefly summarizes the different case studies considered for evaluating IES dynamic behavior.

The Modelica language in the Dymola environment is used for developing the IES dynamic model and control. In addition to the *Modelica Standard Library*, we also use other dependencies for different component models. These include the aforementioned *Hybrid/NHES*, *WindPowerPlants*, and *PhotoVoltaics* libraries. The nominal rating for each SMR module is 160 MW, and the electrical power rating of the BOP with three such modules is 171 MW. The HTSE plant has a nominal rating of 51 MW, with a 21 MW minimum power limit. The wind plant and solar plant considered in our models are rated at 40 and 35 MW, respectively. The wind plant is composed of 24 wind turbines each, rated at 1.7 MW. The focus of our paper is to model the physical behavior and implement the control and coordination of components to meet the demand, while satisfying physical and operational constraints of components. Therefore, a techno-economic planning and operational scheduling is beyond the scope of this paper. However, considering the ease of modification and extension provided by the Modelica language, the IES model can be customized if physical plant data are available.

An upcoming project in Duval County Texas, now named Hydrogen City,[41] considers a large-scale hydrogen production, storage, and distribution infrastructure incorporating solar and wind energy. Although the project is still in its initial stages, this opens a new venue for conceptualizing the proposed IES notion. Hence, for validating the load following capability, we have acquired the data with atmospheric conditions for this particular location. A representative windy day in the month of May 2010 and a sunny day in August 2010 have been considered to provide the wind speed and irradiance input into the wind and solar plant, respectively. The wind speed data for Duval County is acquired by plugging in the corresponding coordinates into the python API of Wind Integration National Dataset (WIND) Toolkit,[42] and the solar irradiance data are derived by using the location in the PySAM (Python for System Advisor Model).[43] Additionally, the grid demand data are obtained from the ACTIVSg2000 Texas test network,[44] where the values have been suitably scaled to match the maximum capacity of IES.

TABLE II. A summary of the different case studies considered for evaluating IES dynamic behavior.

	Generators			Load/demand	
Case	Nuclear	Wind	Solar	Grid	HTSE
A	✓	✗	✗	✓	✗
B	✓	✗	✗	✓	✓
C	✓	✓	✗	✓	✗
D	✓	✗	✓	✓	✗
E	✓	✓	✗	✓	✓
F	✓	✗	✓	✓	✓

A. Electricity production using nuclear energy

The SMR units that function as the primary heat supply system is considered as the sole energy producing resource in this configuration. The thermal energy from the reactor drives the turbine-generator set in the BOP to produce electricity, which is then supplied to the grid through the electrical interconnections in the switch yard. The grid demand on the IES here is to be met by energy conversion in the BOP alone. Therefore, the variations in grid demand corresponds to changes in the BOP power, while the SMRs operate at nominal operating conditions. This is ensured by the steady state control on the individual SMR modules, and the power and pressure control within the BOP subsystem, which enables the IES to follow the demand. To evaluate and analyze the IES operation and control in this configuration, we consider three different cases, i.e., nominal power production, step change in electricity demand, and daily load following operation.

In the case considering nominal power production, the nuclear reactor units generate nominal thermal power, which is 160 MWt for each individual SMR. The BOP further utilizes the thermal energy produced by the three reactor modules to generate electrical power of 171 MW, which is approximately 35% of the steam energy. The physical state of the various IES components during the nominal operation is presented in Fig. 4.

As seen in Fig. 4(a), the SMRs are each operated at nominal thermal power to produce electric power of 171 MW, which is supplied to the grid. In this case, the IES is considered as a baseload generator to the grid. The mixed steam, which flows from the reactor modules to the EM, is directly transferred to the BOP as shown by the mass flow rate in Fig. 4(b). The specific enthalpy of the steam inflow and outflow to the BOP in Fig. 4(c) is indicative of the steam energy being utilized for energy conversion. Since the BOP is operating at nominal conditions, almost all the steam in BOP is directed toward the turbine, as illustrated in Fig. 4(d), where the mass flow rate through the TCV almost equals to the BOP inlet mass flow rate [seen in Fig. 4(b)], while that through BV is close to zero. The reactivity of the core, as illustrated in Fig. 4(e), for each of the three SMR modules increases from zero, representing active thermal power generation, which is further maintained by the steady state controller. The relative temperature between hot leg and cold leg of the reactor is also controlled by the steady state control. The specific enthalpy and the pressure of the high pressure (inlet) and low pressure (outlet) of the turbine is presented in Fig. 4(f).

For a step change in the grid demand, we evaluate the IES control and dynamic behavior, the results of which are presented in Fig. 5. The SMR modules are operated at nominal conditions by the steady state controller, however, the BOP power generation follows the step change in the grid demand as shown in Fig. 5(a). The associated mass

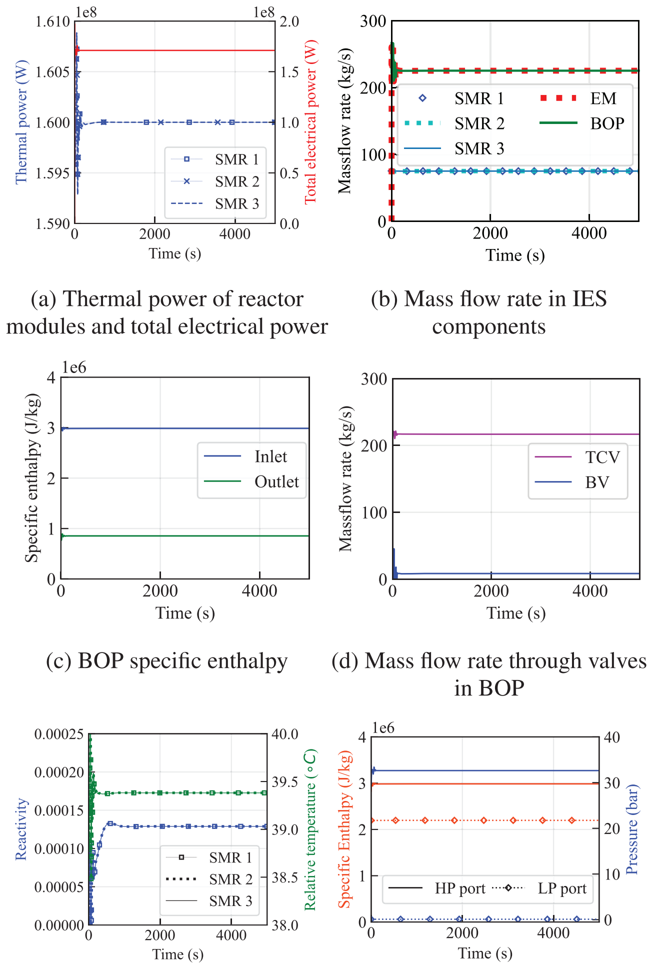

(a) Thermal power of reactor modules and total electrical power (b) Mass flow rate in IES components (c) BOP specific enthalpy (d) Mass flow rate through valves in BOP (e) Core reactivity of reactor modules (f) Steam conditions of turbine HP and LP ports

FIG. 4. Case A1: nominal power production mode.

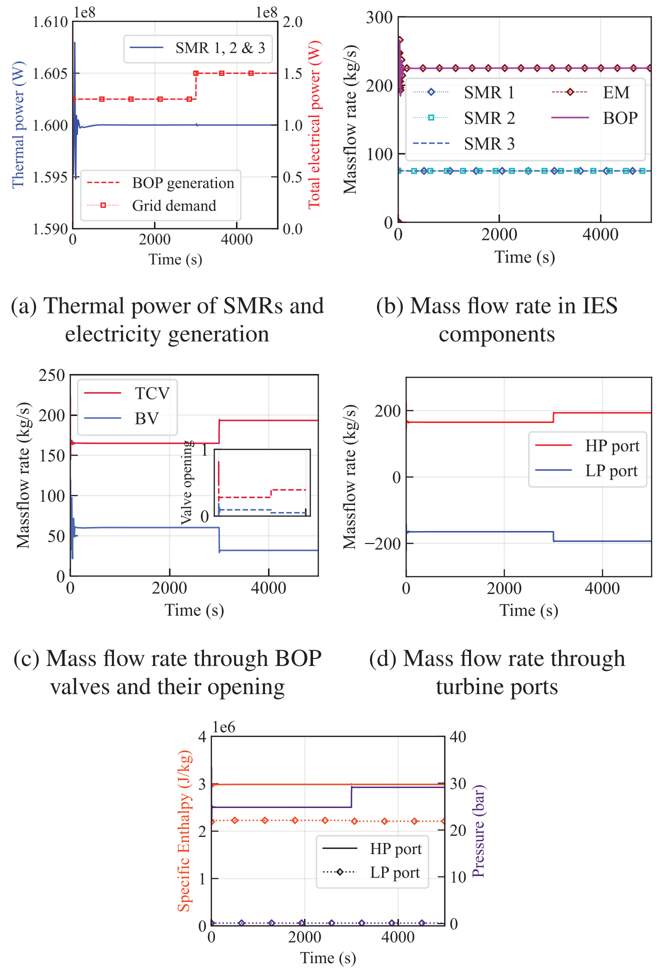

(a) Thermal power of SMRs and electricity generation (b) Mass flow rate in IES components (c) Mass flow rate through BOP valves and their opening (d) Mass flow rate through turbine ports (e) Steam conditions of turbine HP and LP ports

FIG. 5. Case A2: step change in electricity demand.

flow rate in Fig. 5(b) shows that all the steam is directed by the EM toward the BOP as with nominal power production [Fig. 4(b)]. However, once the steam enters the BOP, the mass flow rate toward the turbine is controlled using the TCV in accordance with the power generation required, and the remaining steam energy is diverted through the BV opposing control. This is illustrated in Fig. 5(c). The steam flow through the turbine is shown in Fig. 5(d), which is equal to that through the TCV. The negative mass flow through the LP port simply indicates an outgoing flow. The steam conditions within the turbine are shown in Fig. 5(e). Although the bypass valve regulates the pressure of the secondary coolant (inlet steam to BOP), the pressure variations occur as a result of the power and pressure valve controls in the stream toward the turbine and across the bypass stream. This pressure change is reflected in the entry of steam at the turbine HP port seen in Fig. 5(e). As opposed to the nominal power production case, here, due to changes in the mass flow rate through the HP port, the steam pressure also reflects this variation (also same as power profile) for a constant pressure and specific enthalpy of return supply from BOP.

A representative grid demand over a day is presented in Fig. 6(a). As seen in the figure, the BOP set point and the corresponding generation vary in accordance with the demand. The resulting control on the BOP and the mass flow rate through the TCV and BV are illustrated in Fig. 6(b). This shows that the IES is able to faithfully follow and supply the grid demand. Power and pressure regulation by using bypass steam is a common practice used for steam turbines.[45] The steam bypass is a necessary safety mechanism for regulating steam pressure, while ensuring stable power output, which also prevents damage and wear out of the turbine. However, in terms of efficient utilization of thermal energy, since the energy in the bypass stream is lost and not utilized, it is desirable to minimize bypass flow.

B. Electricity and hydrogen production using nuclear energy

In this case, we consider the SMRs to supply the thermal energy for both electricity generation and hydrogen production. The steady

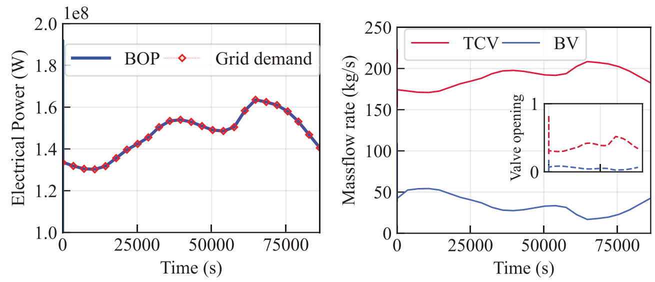

(a) Power profile (b) Mass flow rate within BOP

FIG. 6. Case A3: daily demand supplied by BOP.

state controller within the SMR modules and the valve controls (TCV and BV) are in operation to meet the setpoint on the BOP, while the SMRs are maintained at nominal condition. We consider two cases to illustrate the two control modes, i.e., steam control and power control associated with the HTSE plant.

In the first case with steam control, supplying the grid demand is considered as the primary goal of the IES, with the optimal grid dispatch signals available to the supervisory controller (SC). The SC then sends suitable setpoints to individual plants. From the electrical power perspective, the hydrogen plant is a flexible load and, hence, the SC determines the electrical setpoint for HTSE (as load). Given that the electrical power is predefined, the HTSE plant internal control operates in the steam control mode to ensure that sufficient temperatures are achieved for electrolysis. The results of this simulation are presented in Fig. 7.

As seen in Fig. 7(a), the BOP supplies the electrical power demand of both the HTSE and the grid. Hence, here, the BOP is operating at its nominal value. The BOP setpoint and actual generation, and the grid setpoint and actual supply are shown in positive values, while the HTSE setpoint and power profiles are shown as negative in the figure to indicate power consumption. As seen in the figure, when the grid demand increases, the HTSE consumes less power and vice versa. The hydrogen plant, therefore, acts as a flexible or variable electric load in the IES. In Fig. 7(b), it is seen that the steam is split in the EM into two, one stream toward BOP and the other toward the HTSE. The steam flow into HTSE also follows the power profile. The HTSE control is illustrated in Figs. 7(c) and 7(d). The total HTSE power is used in the SOEC stacks and also for heating the anode and cathode (H_2) stream as shown in Fig. 7(c). The steam flow control ensures that the cathode (and anode) gas temperature is maintained at 850 °C as illustrated in Fig. 7(d). The cathode gas without heating and with heating represented in the figure are the streams on either sides of heat recuperator. Since the BOP is operating at the nominal value, as seen in Fig. 7(e), steam is mostly directed through TCV to steam turbine for electricity generation, while the bypass steam is close

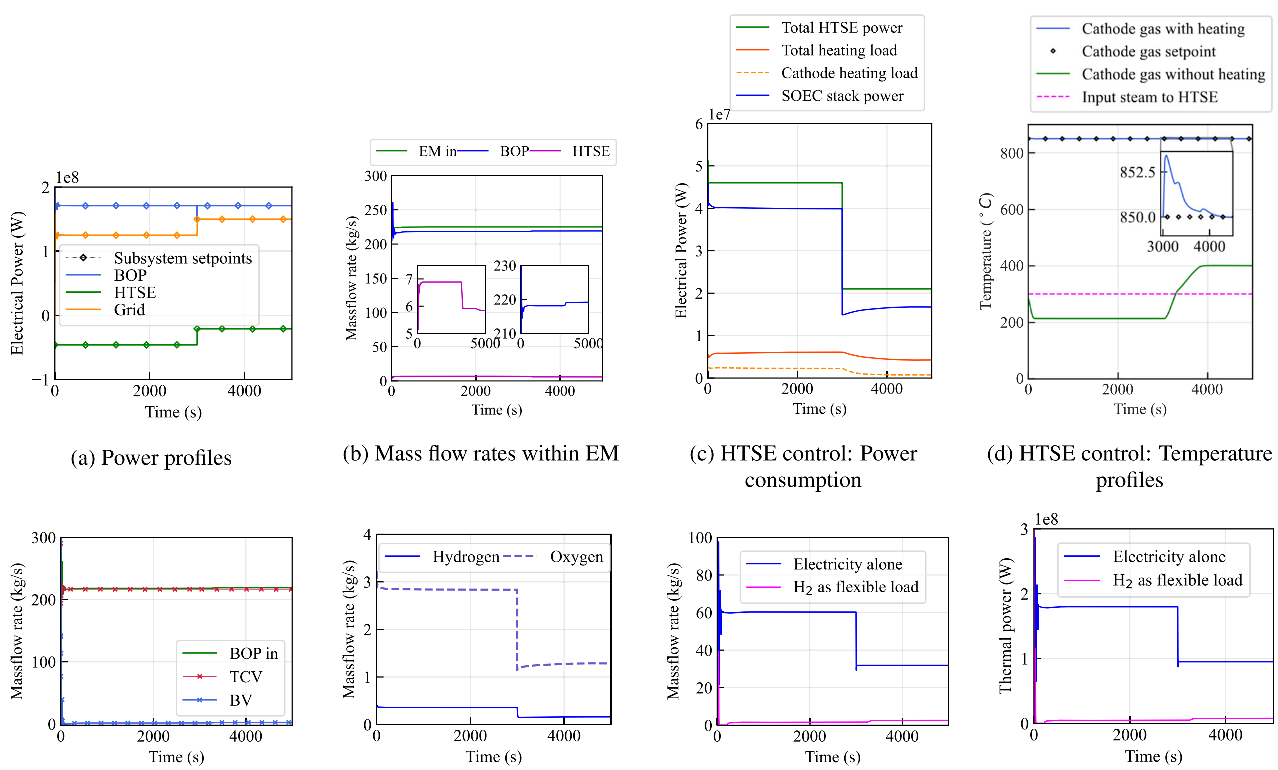

(a) Power profiles (b) Mass flow rates within EM (c) HTSE control: Power consumption (d) HTSE control: Temperature profiles

(e) Mass flow rates within BOP (f) H_2 and O_2 production rates (g) Comparison with case A2: BV mass flow rate (h) Comparison with case A2: BV thermal power flow

FIG. 7. Case B1: step change in electricity demand with HTSE as flexible load.

to zero. The hydrogen and oxygen production rates of the HTSE are presented in Fig. 7(f), and it follows the electric power input [Fig. 7(a)] and thermal input [Fig. 7(b)], i.e., increase in HTSE power results in more hydrogen production.

In Fig. 7(g), we compare case A2 with no HTSE plant and case B1 with HTSE for the same step change in the grid demand. As observed in the figure, the steam diverted through the bypass valve (BV) is close to zero for case B1, while the surplus energy is bypassed in case A2. The bypass steam is dumped into the condenser to regulate the secondary coolant pressure while following the grid demand. Thus, the thermal energy carried in this stream is wasted. With the inclusion of hydrogen as an end product, however, the bypass steam is reduced, resulting in better utilization of thermal energy and improved efficiency. The thermal power flow through the BV is also similarly compared in Fig. 7(h).

In the case where the dispatch of thermal energy is available to the SC, the EM apportions the steam to BOP and HTSE accordingly using valve control. The results of this case are presented in Fig. 8. With the given steam input to the HTSE, the power control within the module determines the power consumption set point. This power is utilized for electrolysis in the SOEC and heating the cathode and anode streams shown in Figs. 8(c) and 8(d). The step decrease in steam mass flow results in a proportional decrease in electrolysis power, i.e., the power consumed by the SOEC stack [Fig. 8(c)]. However, with the decrease in thermal energy, the electrical heating increases to achieve the desired operating temperature [Fig. 8(d)].

C. Electricity production using nuclear and wind energy

In this configuration, the wind power plant is present in the IES in addition to the SMR modules for supplying the grid demand.

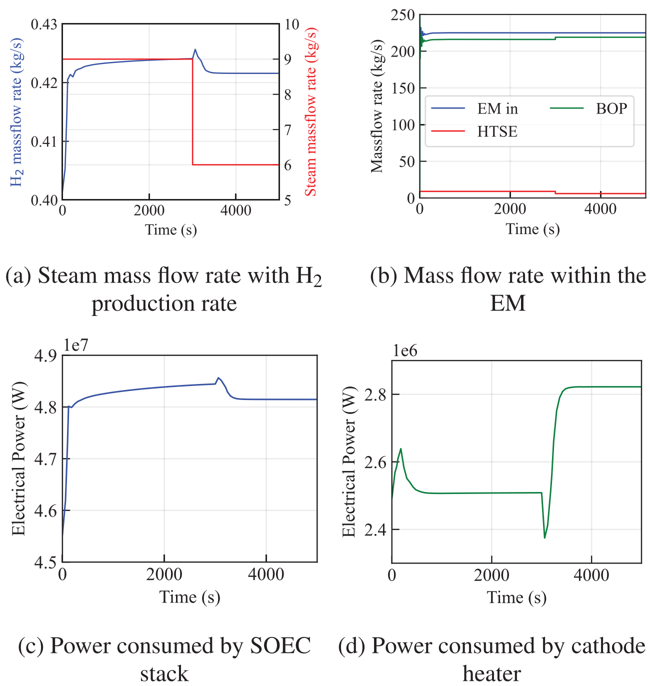

(a) Steam mass flow rate with H_2 production rate
(b) Mass flow rate within the EM
(c) Power consumed by SOEC stack
(d) Power consumed by cathode heater

FIG. 8. Case B2: step change in steam input to HTSE (power control mode).

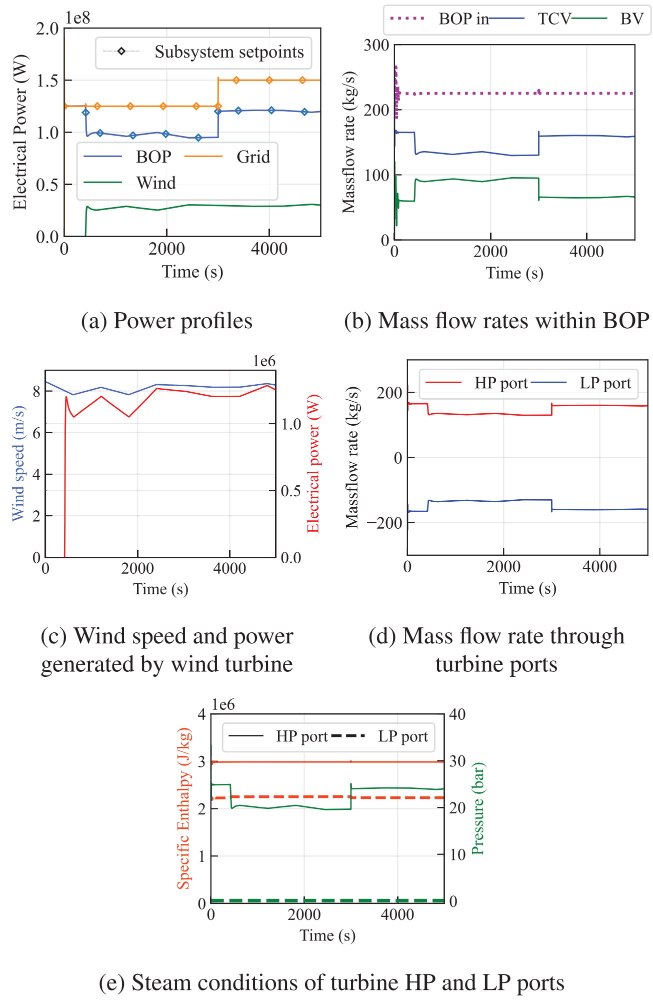

(a) Power profiles
(b) Mass flow rates within BOP
(c) Wind speed and power generated by wind turbine
(d) Mass flow rate through turbine ports
(e) Steam conditions of turbine HP and LP ports

FIG. 9. Case C: step change in electricity demand with wind power generation.

The different observations from this case study are presented in Fig. 9. The step change in grid demand here is the same as those in the previous cases. As seen in Fig. 9(a), since the wind energy is non dispatchable, it is directly used for supplying the grid demand, while the BOP meets the remaining requirement by varying its generation. This is performed by controlling the steam flow toward the turbine by TCV and diverting the rest toward the condenser by BV, as seen in Fig. 9(b). The wind speed and the equivalent power generated by a single wind turbine generator unit is represented in Fig. 9(c). The wind power output of the plant in Fig. 9(a) is considerably smoothened due to the presence of multiple turbines. The pitch control ensures the optimum power coefficient for electric power production by controlling the pitch angle. Accordingly, the pitch control module estimates the optimum coefficient to be at a tip speed of 7.8 m/s. The mass flow rate through the steam turbine ports in BOP, i.e., HP (inlet) and LP (outlet), are shown in Fig. 9(d). This is the same as that of TCV [Fig. 9(b)], and the negative sign here indicates outgoing steam flow. The steam conditions illustrated in Fig. 9(e) represent that the steam at high pressure port enters the turbine corresponding to the power profile and TCV mass flow rate. The return supply from the turbine is at a minimum constant pressure. Therefore, the different controls within the IES ensure that the wind power is utilized to supply the demand, while relying on the BOP to provide required flexibility.

D. Electricity production using nuclear and solar energy

In this configuration, the solar energy plant is used to supply the grid demand alongside the SMR modules as the primary energy resource. The simulation results of this case study are presented in Fig. 10. The nondispatchable solar power produced is supplied to the grid, while the BOP functions as the flexible generating resource, as illustrated in Fig. 10(a). The steam flow directed toward the turbine (through TCV) and the bypassed steam (through BV) both follow the profile of the BOP to generate the required power as observed in Fig. 10(b). The irradiance profile and the corresponding power produced by a unit in the solar plant is presented in Fig. 10(c). As seen in Fig. 10(d), the steam flow through the turbine ports reflects the power generation required, which is also an effect of the TCV and BV control. Also, in Fig. 10(e), it is seen that the pressure of the steam supply at the HP (inlet) port of the turbine follows the electricity generation required from the BOP. Therefore, this study shows that the solar power generation can be utilized to supply the grid demand, while the BOP provides the flexibility to accommodate solar energy.

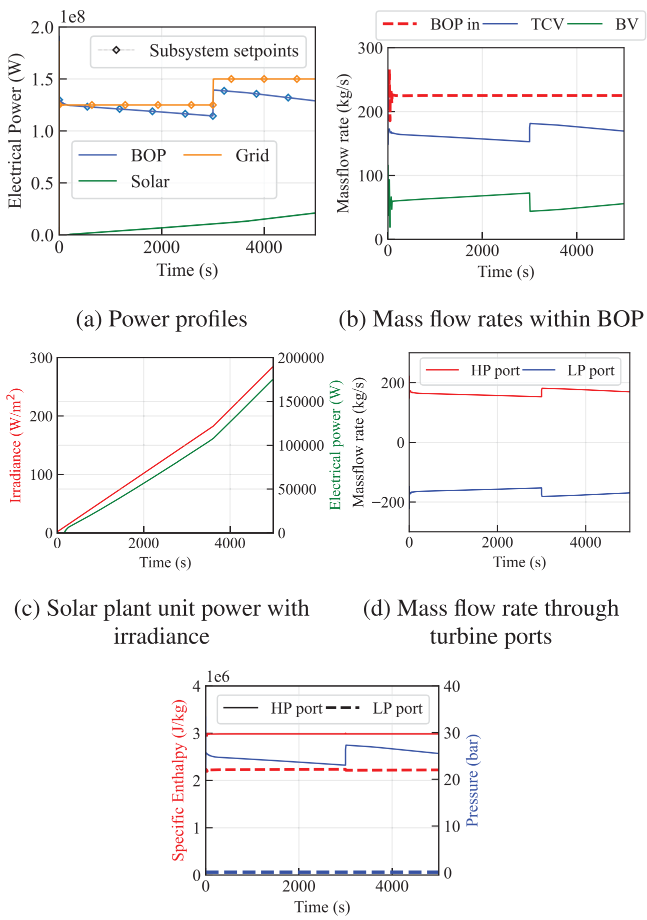

(a) Power profiles (b) Mass flow rates within BOP

(c) Solar plant unit power with irradiance (d) Mass flow rate through turbine ports

(e) Steam conditions of HP and LP ports in the turbine

FIG. 10. Case D: Step change in electricity demand with solar power generation.

E. Electricity and hydrogen production using nuclear and wind energy

This configuration is the proposed IES architecture where the SMR modules and the wind energy resource supply the grid demand while also producing hydrogen. The different facets of the IES integration and dynamics can be validated in this case study, such as the presence of variable renewables and the generation of hydrogen as an end product. Two case studies are performed here. In the first scenario, a step change in grid demand as in the previous case studies is considered. In the second scenario, a daily pattern of grid demand and wind speed are provided as input to observe the load following capability of the designed control architecture.

The step change in grid demand and the resulting IES behavior are presented in Fig. 11. When the grid demand or dispatch of the tightly coupled IES to the grid is provided, the BOP capacity along with the non-dispatchable wind is available for utilization. The control strategy in Sec. III G ensures that the steam energy utilization is maximized. Therefore, the electrical energy requirement of the HTSE and grid are first supplied by the wind and then the flexible BOP as seen in Fig. 11(a). The wind profile in Fig. 9(c) is applied here as well. It is observed that the surplus electrical energy from the wind plant and the BOP, while satisfying the grid demand, is directed toward the HTSE up to the maximum operating limit of 51 MWe. Following this, the BOP adjusts power generation based on wind availability and grid demand. The HTSE, therefore, provides the flexibility of absorbing variations up to 51 MWe for the BOP. The thermal energy from the SMR modules is also supplied to the HTSE for hydrogen production which is maximum in this case. The remnant BOP generation is seen to follow the grid demand. The BOP offers flexibility in generation, while the hydrogen plant offers flexibility in consumption for the specified grid demand and wind power.

The corresponding mass flow rates through the different components are shown in Fig. 11(b). The power profile dictates the mass flow rate through the TCV and BV, which is shown in Fig. 11(c). As seen in Fig. 11(d), the hydrogen production rate is at its nominal value of 0.4 kg/s for the duration with wind power generation. In Fig. 11(e), the IES configuration producing electricity and hydrogen with a wind plant and the configuration without a wind plant (case B1) are compared. The mass flow rate into HTSE represented in the figure indicates that with surplus wind power generation, the hydrogen plant is utilized at its nominal capacity, while in the case without wind generation, the hydrogen plant acts as a flexible load in association with the grid demand.

Figure 12 illustrates the capability of IES to follow the grid demand over a period of 24 h with varying wind power generation. As seen in Fig. 12(a), wind power and the BOP supplies the grid while producing hydrogen at the rated power. The equivalent hydrogen and oxygen produced is presented in Fig. 12(b).

F. Electricity and hydrogen production using nuclear and solar energy

Similar to the previous case, the grid demand is supplied by the SMR modules with hydrogen as a by-product. However, here the

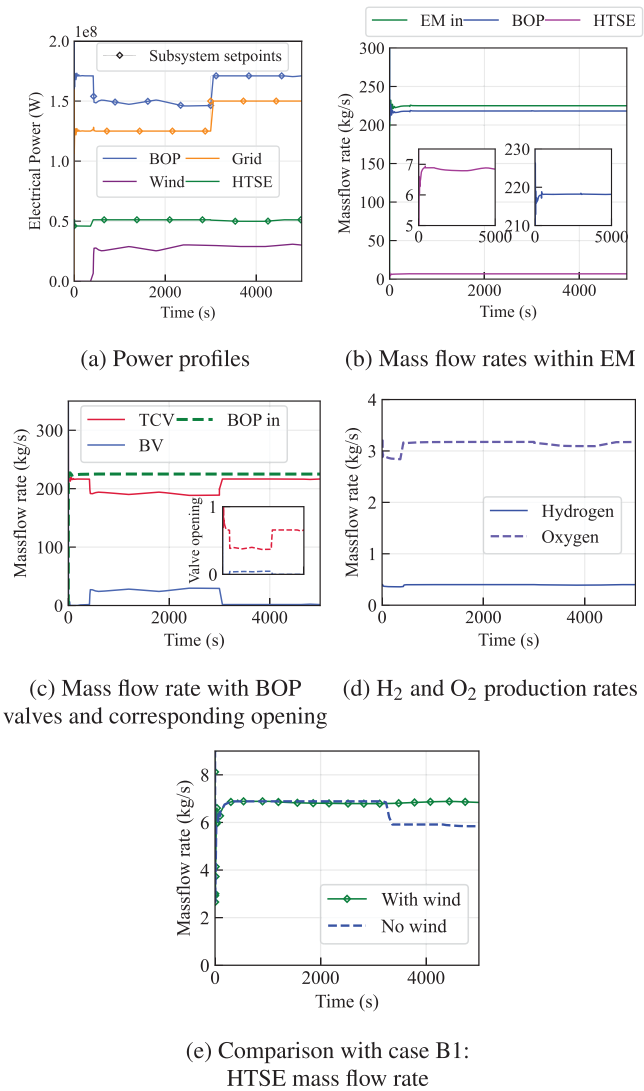

(a) Power profiles (b) Mass flow rates within EM

(c) Mass flow rate with BOP valves and corresponding opening (d) H_2 and O_2 production rates

(e) Comparison with case B1: HTSE mass flow rate

FIG. 11. Case E1: step change in electricity demand with wind power generation and HTSE as flexible load.

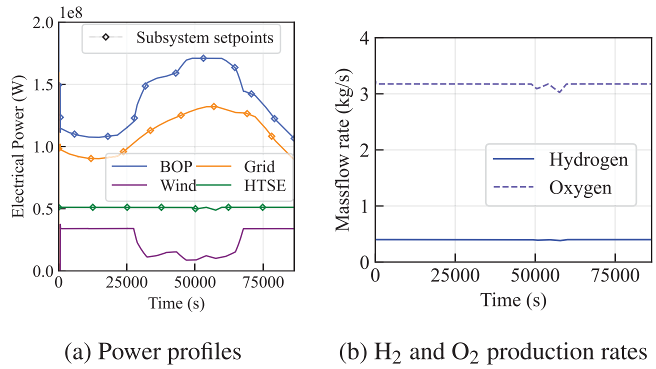

(a) Power profiles (b) H_2 and O_2 production rates

FIG. 12. Case E2: grid demand and wind power generation varying over a day.

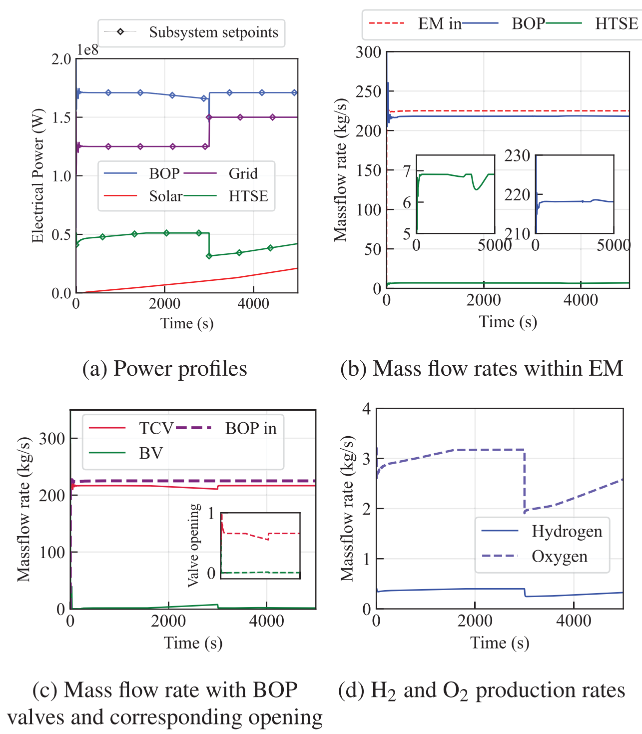

(a) Power profiles (b) Mass flow rates within EM

(c) Mass flow rate with BOP valves and corresponding opening (d) H_2 and O_2 production rates

FIG. 13. Case F1: step change in electricity demand with solar power generation and HTSE as flexible load.

renewable resource is the solar plant. Two case studies, one with step change in grid demand and the other with daily solar and grid demand pattern, are performed.

The results of the case with step change in grid demand are presented in Fig. 13. In contrast to the wind case study, here, the power produced by the solar plant is a slowly rising ramp as illustrated in Fig. 13(a). Since the minimum HTSE power operating limit is 21 MW, the solar power is not sufficient for direct hydrogen production, and up to 3000 s, the BOP supplies both the grid demand and the HTSE. Once the step change occurs at 3000 s, the BOP power set point is increased till its maximum value as observed in the figure. Thereafter, in order to support the grid, the power to HTSE is decreased. However, the HTSE follows the solar power profile. The mass flow rate into HTSE shown in Fig. 13(b) is controlled to achieve the desired temperature using steam control mode of HTSE. The valves in the BOP operate in accordance with BOP power setpoint as represented in Fig. 13(c). The hydrogen and oxygen production rates in Fig. 13(d) are a direct result of the variation in the input power supplied to the HTSE for hydrogen production.

For a daily demand pattern on the IES, with varying solar power generation, the supervisory control generates the setpoints for the operation of the BOP and HTSE, which are shown in Fig. 14(a). As expected, the net demand on the IES decreases during the presence of solar generation. The BOP supplies the nominal power to HTSE, while also following the grid demand. The hydrogen and oxygen production rates in Fig. 14(b) reflect the trend of HTSE power profile.

Each IES component is prescribed safe limits of operation, which depend on several factors such as the type and design of components

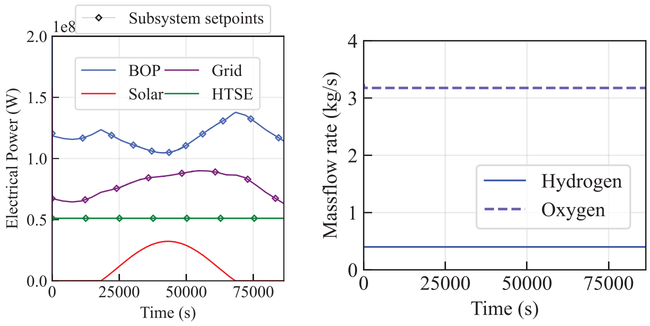

(a) Power profiles (b) H_2 and O_2 production rates

FIG. 14. Case F2: grid demand and solar power generation varying over a day.

(including geometrical and physical properties), type of medium, etc. These descriptions are already embedded into the component models derived from the existing libraries, which are developed from real-world device designs. For instance, in the case of SMRs, there exist a limit on operating temperature to avoid the risk of meltdown, a safe pressure range to prevent rupture of the reactor vessel, and a limit on thermal power output[21,24] as discussed in the paper. Meanwhile, the BOP has limits on steam conditions (e.g., temperature, pressure, and flow rate), maximum electrical power output, etc. The HTSE, on the other hand, has operational temperature and pressure ranges and limit on the maximum electrical power drawn to prevent damage to the electrolysis cell.[21,30] Therefore, the IES exhibits the load-following capability while satisfying these operational constraints imposed for safety and efficiency.

V. CONCLUSION

A dynamic model of an integrated energy system with nuclear and renewable energy resources supplying energy to the power grid with hydrogen as a by-product was developed in this study. Along with the physics-based component description, a control architecture for energy management within the IES was also designed to respond to the grid dispatch signals. The control and coordination of the different subsystems and their dynamic response in terms of the thermal-fluid behavior, energy flow, etc., were validated by considering different configurations and modes of operation. From the different operational scenarios considered on multiple configurations, it can be concluded that the IES

1. provides flexibility while utilizing the thermal energy from the nuclear process to supply both the electrical grid and the hydrogen gas production system (HTSE);
2. efficiently accommodates the wind and solar power to meet the demand of the electric grid while relying on hydrogen as flexible load and nuclear (with balance of plant) as flexible generation;
3. effectively responds to variation in demands by diverting flow to alternative energy paths; and
4. exhibits stable load-following capability without perturbations during normal operation and in the presence of varying renewable generation. This indicates that the various component controllers in the IES work harmoniously with the supervisory control to ensure that the grid demand is satisfied in a multi-energy, multi-product system.

With the physical system effectively modeled and the control architecture validated, the eventual extension of this work could consider integrating the information derived from optimal planning and operation tools into the physical system representation. This implies that in the future, the IES design and configuration from techno-economic analysis tools will be used to scale up/down or build units. Additionally, the optimal dispatch signals acquired from operation scheduling tools (i.e., multi-timescale, unit-commitment, economic dispatch models[46]) will be fed into the supervisory controller as demand inputs. Other potential work on the modeling front includes developing a hydrogen facility model for utilization of the clean hydrogen using storage tanks, fuel cells, etc., and capturing the dynamics of the grid using detailed power grid and generator modeling.

ACKNOWLEDGMENTS

This material is based upon work supported by two awards: (i) the U.S. Department of Energy under Award No. DE-NE0008899, and (ii) award through the INL Laboratory Directed Research & Development (LDRD) Program under DOE Idaho Operations Office Contract No. DE-AC07-05ID14517.

AUTHOR DECLARATIONS

Conflict of Interest

The authors have no conflicts to disclose.

Author Contributions

Roshni Anna Jacob: Data curation (equal); Formal analysis (equal); Investigation (equal); Methodology (equal); Software (equal); Validation (equal); Visualization (equal); Writing – original draft (equal). **Jie Zhang:** Conceptualization (equal); Funding acquisition (equal); Investigation (equal); Methodology (equal); Project administration (equal); Supervision (equal); Writing – review & editing (equal).

DATA AVAILABILITY

The data that support the findings of this study are available from the corresponding author upon reasonable request.

REFERENCES

[1]H. E. Garcia, J. Chen, J. S. Kim, M. G. McKellar, W. R. Deason, S. M. Bragg-Sitton, and R. D. Boardman, "Nuclear hybrid energy systems regional studies: West Texas & Northeastern Arizona," Technical Report No. INL/EXT-15-34503 [Idaho National Laboratory (INL), Idaho Falls, ID, 2015].
[2]M. S. Greenwood, S. M. Cetiner, T. J. Harrison, and D. Fugate, "A templated approach for multi-physics modeling of hybrid energy systems in Modelica," Technical Report No. ORNL/TM-2018/757 [Oak Ridge National Laboratory (ORNL), Oak Ridge, TN, 2017].
[3]S. M. Bragg-Sitton, R. Boardman, C. Rabiti, and J. O'Brien, "Reimagining future energy systems: Overview of the us program to maximize energy utilization via integrated nuclear-renewable energy systems," Int. J. Energy Res. **44**, 8156–8169 (2020).
[4]M. Ruth, D. Cutler, F. Flores-Espino, and G. Stark, "The economic potential of nuclear-renewable hybrid energy systems producing hydrogen," Technical Report [National Renewable Energy Laboratory (NREL), Golden, CO, 2017].
[5]S. M. Cetiner, M. S. Greenwood, T. J. Harrison, A. L. Qualls, A. G. Yigitoglu, and D. L. Fugate, *Nuclear Hybrid Energy Systems FY16 Modeling Efforts at ORNL* (Oak Ridge National Laboratory, Oak Ridge, TN, 2016).

[6]D. Michaelson and J. Jiang, "Review of integration of small modular reactors in renewable energy microgrids," Renewable Sustainable Energy Rev. **152**, 111638 (2021).
[7]S. McQueen, J. Stanford, S. Satyapal, E. Miller, N. Stetson, D. Papageorgopoulos, N. Rustagi, V. Arjona, J. Adams, K. Randolph *et al.*, "Department of energy hydrogen program plan," Technical Report No. DOE/EE-2128 [US Department of Energy (USDOE), Washington DC, 2020].
[8]M. F. Ruth, P. Jadun, and B. S. Pivovar, "H2@ scale: Technical and economic potential of hydrogen as an energy intermediate," Technical Report No. NREL/PR-6A20-70456 [National Renewable Energy Laboratory (NREL), Golden, CO, 2017].
[9]A. Chandrasekar, D. Flynn, and E. Syron, "Operational challenges for low and high temperature electrolyzers exploiting curtailed wind energy for hydrogen production," Int. J. Hydrogen Energy **46**, 28900–28911 (2021).
[10]S. T. Revankar, "Nuclear hydrogen production," in *Storage and Hybridization of Nuclear Energy* (Elsevier, 2019), pp. 49–117.
[11]F. Ruiming, "Multi-objective optimized operation of integrated energy system with hydrogen storage," Int. J. Hydrogen Energy **44**, 29409–29417 (2019).
[12]J. Rahman, R. A. Jacob, and J. Zhang, "Harnessing operational flexibility from power to hydrogen in a grid-tied integrated energy system," in *International Design Engineering Technical Conferences and Computers and Information in Engineering Conference* (American Society of Mechanical Engineers, 2022), Vol. 86229.
[13]P. W. Talbot, D. J. McDowell, J. D. Richards, J. J. Cogliati, A. Alfonsi, C. Rabiti, R. D. Boardman, S. Bernhoft, F. d l Chesnaye, E. Ela *et al.*, "Evaluation of hybrid FPOG applications in regulated and deregulated markets using HERON," Technical Report No. INL/EXT-20-60968 [Idaho National Laboratory (INL), Idaho Falls, ID, 2020].
[14]H. Li, J. Rahman, and J. Zhang, "Optimal planning of co-located wind energy and hydrogen plants: A techno-economic analysis," J. Phys.: Conf. Ser. **2265**, 042063 (2022).
[15]J. Wu, X. Chen, S. Badakhshan, J. Zhang, and P. Wang, "Spectral graph clustering for intentional islanding operations in resilient hybrid energy systems," IEEE Trans. Ind. Inf. **19**, 5956–5964 (2022).
[16]B. Poudel and R. Gokaraju, "Small modular reactor (SMR) based hybrid energy system for electricity and district heating," IEEE Trans. Energy Convers. **36**, 2794–2802 (2021).
[17]R. A. Jacob, J. Rahman, and J. Zhang, "Dynamic modeling and simulation of integrated energy systems with nuclear, renewable, and district heating," in *North American Power Symposium (NAPS)* (IEEE, 2021).
[18]S. E. Mattsson, H. Elmqvist, and M. Otter, "Physical system modeling with Modelica," Control Eng. Practice **6**, 501–510 (1998).
[19]K. Frick, S. Bragg-Sitton, and C. Rabiti, "Modeling the Idaho National Laboratory thermal-energy distribution system (TEDS) in the Modelica ecosystem," Energies **13**, 6353 (2020).
[20]M. S. Greenwood, R. Hale, L. Qualls, S. Cetiner, D. Fugate, and T. Harrison, "Transform-transient simulation framework of reconfigurable models," Technical Report [Oak Ridge National Laboratory (ORNL), Oak Ridge, TN, 2017].
[21]K. L. Frick, A. Alfonsi, C. Rabiti, and D. M. Mikkelson, "Hybrid user manual," Technical Report No. INL/MIS-20-60624-Rev001 [Idaho National Laboratory (INL), Idaho Falls, ID, 2022].
[22]A. Alfonsi, A. Epiney, C. Rabiti, J. S. Kim, K. Frick, *et al.*, see https://github.com/idaholab/HYBRID for "HYBRID."
[23]D. Mikkelson, C.-W. Chang, S. M. Cetiner, A. L. Qualls, J. M. Doster, and T. N. Dinh, "Small modular reactor modeling using Modelica for nuclear-renewable hybrid energy systems applications," Trans. Am. Nucl. Soc. **113**, 903–906 (2015).
[24]K. L. Frick, "Status report on the NuScale module developed in the Modelica framework," Technical Report No. INL/EXT-19-55520-Rev000 [Idaho National Laboratory (INL), Idaho Falls, ID, 2019].
[25]C. Rabiti, A. Epiney, P. Talbot, J. Kim, S. Bragg-Sitton, A. Alfonsi, A. Yigitoglu, S. Greenwood, S. Cetiner, F. Ganda *et al.*, "Status report on modelling and simulation capabilities for nuclear-renewable hybrid energy systems," Technical Report No. INL/EXT-17-43441 [Idaho National Laboratory (INL), Idaho Falls, ID, 2017].
[26]H. E. Garcia, J. Chen, J. S. Kim, R. B. Vilim, W. R. Binder, S. M. B. Sitton, R. D. Boardman, M. G. McKellar, and C. J. Paredis, "Dynamic performance analysis of two regional nuclear hybrid energy systems," Energy **107**, 234–258 (2016).
[27]J. Chen, H. E. Garcia, J. S. Kim, and S. M. Bragg-Sitton, "Operations optimization of nuclear hybrid energy systems," Nucl. Technol. **195**, 143–156 (2016).
[28]A. S. Epiney, C. Rabiti, P. W. Talbot, J. S. Kim, S. M. Bragg-Sitton, and J. Richards, "Case study: Nuclear-renewable-water integration in Arizona," Technical Report [Idaho National Laboratory (INL), Idaho Falls, ID, 2018].
[29]J. S. Kim, M. McKellar, S. M. Bragg-Sitton, and R. D. Boardman, "Status on the component models developed in the Modelica framework: High-temperature steam electrolysis plant & gas turbine power plant," Technical Report No. INL/EXT-16-40305 [Idaho National Laboratory (INL), Idaho Falls, ID, 2016].
[30]J. S. Kim, S. M. Bragg-Sitton, and R. D. Boardman, "Status report on the high-temperature steam electrolysis plant model developed in the Modelica framework (FY17)," Technical Report No. INL/EXT-17-43056 [Idaho National Laboratory (INL), Idaho Falls, ID, 2017].
[31]J. S. Kim, R. D. Boardman, and S. M. Bragg-Sitton, "Dynamic performance analysis of a high-temperature steam electrolysis plant integrated within nuclear-renewable hybrid energy systems," Appl. Energy **228**, 2090–2110 (2018).
[32]J. O'brien, J. Hartvigsen, R. Boardman, J. Hartvigsen, D. Larsen, and S. Elangovan, "A 25 kw high temperature electrolysis facility for flexible hydrogen production and system integration studies," Int. J. Hydrogen Energy **45**, 15796–15804 (2020).
[33]R. D. Boardman, T. L. Westover, S. J. Remer, and J. Cadogan, "Plan for scaling up hydrogen production with nuclear power plants," Technical Report No. INL/RPT-22-68155-Rev000 [Idaho National Laboratory (INL), Idaho Falls, ID, 2022].
[34]Bloomenergy, see https://www.bloomenergy.com/news/idaho-national-lab-and-bloom-energy-produce-hydrogen-at-record-setting-efficiencies/ for "Idaho National Laboratory and Bloom Energy Produce Hydrogen at Record-Setting Efficiencies" (2022).
[35]R. Pinsky, P. Sabharwall, J. Hartvigsen, and J. O'Brien, "Comparative review of hydrogen production technologies for nuclear hybrid energy systems," Prog. Nucl. Energy **123**, 103317 (2020).
[36]K. L. Frick, P. W. Talbot, D. S. Wendt, R. D. Boardman, C. Rabiti, S. M. Bragg-Sitton, M. Ruth, D. Levie, B. Frew, A. Elgowainy *et al.*, "Evaluation of hydrogen production feasibility for a light water reactor in the midwest," Technical Report No. INL/EXT-19-55395-Rev000 [Idaho National Laboratory (INL), Idaho Falls, ID, 2019].
[37]T. A. Ulrich, R. Lew, T. J. Mortenson, J. Park, H. D. Medema, and R. L. Boring, "An integrated energy systems prototype human-system interface for a steam extraction loop system to support joint electricity-hydrogen flexible operations," Technical Report No. INL/EXT-20-57880-Rev000 [Idaho National Laboratory (INL), Idaho Falls, ID, 2020].
[38]P. Eberhart, T. S. Chung, A. Haumer, and C. Kral, "Open source library for the simulation of wind power plants," in *Proceedings of the 11th International Modelica Conference, Versailles, France, September 21–23, 2015* (Linköping University Electronic Press, 2015), Vol. 118, pp. 929–936.
[39]J. Brkic, M. Ceran, M. Elmoghazy, R. Kavlak, A. Haumer, and C. Kral, "Open source photovoltaics library for systemic investigations," in *Proceedings of the 13th International Modelica Conference, Regensburg, Germany, March 4–6, 2019* (Linköping University Electronic Press, 2019), Vol. 157.
[40]IAEA Nuclear Energy Series NP-T-3.23, *Non-baseload operation in nuclear power plants: Load following and frequency control modes of flexible operation* [International Atomic Energy Agency (IAEA), Vienna, 2018].
[41]See https://www.ghi-corp.com/projects/hydrogen-city for "HYDROGEN CITY."
[42]C. Draxl, A. Clifton, B.-M. Hodge, and J. McCaa, "The wind integration national dataset (wind) toolkit," Appl. Energy **151**, 355–366 (2015).
[43]P. Gilman, S. Janzou, D. Guittet, J. Freeman, N. DiOrio, N. Blair, M. Boyd, T. Neises, and M. Wagner, "Pysam (Python wrapper for system advisor model SAM)," Technical Report No. NREL SWR-19-57 [National Renewable Energy Laboratory (NREL), Golden, CO, 2019].
[44]A. B. Birchfield, T. Xu, K. M. Gegner, K. S. Shetye, and T. J. Overbye, "Grid structural characteristics as validation criteria for synthetic networks," IEEE Trans. Power Syst. **32**, 3258–3265 (2016).
[45]R. Aminov, A. Moskalenko, and M. Garievskii, "Using the steam turbines with bypass steam distribution at CCGT for primary frequency control," J. Phys.: Conf. Ser. **1111**, 012047 (2018).
[46]J. Rahman and J. Zhang, "Multi-timescale operations of nuclear-renewable hybrid energy systems for reserve and thermal products provision," J. Renewable Sustainable Energy **15**, 025901 (2023).